Modeling of *n*-butane ignition, combustion, and preflame oxidation in the 20-liter vessel

Frolov S. M.[1], Basevich V. Ya.[1], Smetanyuk V. A.[1], Belyaev A. A.[1], Pasman H. J.[2]
[1]*Semenov Institute of Chemical Physics, Moscow, Russia*
[2]*Delft University of Technology, Delft, The Netherlands*

Abstract

The objective of the study reported herein is mathematical modeling of fuel-rich *n*-butane mixture preparation, ignition, preflame oxidation, and combustion in the standard 20-liter explosion vessel. Based on the CFD simulations of the mixing process and natural convection of the ignition kernel, as well as on the analysis of the detailed reaction mechanism of *n*-butane oxidation, laminar flame propagation, and self-ignition, possible explanations for the phenomena observed experimentally have been suggested. The results of the study indicate that apparently inflammable mixtures can become hazardous depending on the mixture preparation procedure and forced ignition timing.

Introduction

Physical and chemical processes in a standard spherical 20-liter explosion vessel are very complicated. In the experiments [1], a new mixture preparation method was established to study flammability of fuel-rich *n*-butane–oxygen mixtures at elevated temperatures and pressures. A presumably nonflammable *n*-butane–oxygen mixture with the equivalence ratio of 23 was prepared by fast injection of oxygen from the heated and pressurized canister to the heated explosion vessel filled with *n*-butane. The temperature of the setup was continuously supported at 500 K. The pressure in the vessel after completion of oxygen injection was 4.1 bar. The mixture was ignited in the vessel center with different delay times after completion of oxygen injection. Using this method, the authors of [1] observed the influence of the forced ignition delay time (IDT) on the explosion pressure ratio and maximum rate of pressure rise. The explosion pressure ratio was shown to increase from 1.3 at an IDT of 20 s to a maximum of 1.6 at an IDT of 40 s. After the maximum, the explosion pressure ratio dropped with increasing the IDT, reached a minimum of 1.27 at an IDT of 360 s and rose again to a second maximum of 1.4 at an IDT of 1020 s. The maximum rate of pressure rise roughly followed a similar trend. Starting from about 1220 s, the test mixture self-ignited.

Preliminary multidimensional CFD simulations of the mixing process of high- and low-pressure air in the 20-liter vessel have been performed in [2, 3]. It has been shown that the thermochemical conditions at the ignition site in experiments [1] could be affected in the long run by thermal stratification of the matter in the vessel and by the residual oxygen coming from the manifold after injection termination. Thus, in experiments [1], several phenomena occurred simultaneously. These are mixing, forced ignition followed by flame propagation, preflame oxidation, heat transfer, and natural convection.

To understand the relationship between characteristic times and scales of the phenomena, multidimensional CFD simulations of mixture preparation in the vessel, ignition, and flame kernel buoyancy have been performed together with detailed calculations of flame velocity and structure in the fuel-rich *n*-butane–oxygen mixtures at elevated temperature (500 K) and pressure (4.1 bar), relevant to experiments [1].

1. Thermodynamics

The test mixture in [1] contained 78% C_4H_{10} and 22% O_2, which corresponded to the equivalence ratio of $\Phi = 23$, i.e., it was extremely fuel-rich. The mean molecular mass of the test mixture was 52.3767 kg/kmol. Tables 1 and 2 show the results of thermodynamic calculations for the test mixture at $p_0 = 4.1$ bar and $T_0 = 500$ K using the thermochemical

code TDS [4]. Presented in the tables are the thermodynamic temperature T, density r, pressure p, molecular mass m, and species mole fractions at constant-pressure (HP-problem) and constant-volume (UV-problem) combustion of the test mixture at p_0 = 4.1 bar and $T_0 = 500$ K.

According to Table 1, if the test mixture would be flammable, the combustion temperature in the constant-pressure flame could be equal to 911.63 K. According to Table 2, constant-volume combustion of the test mixture would result in the maximal thermodynamic temperature and pressure equal to 1049.42 K and 25.47 bar, respectively, i.e., the thermodynamic pressure ratio could be $p_{\max} / p_0$ = 6.21. The equilibrium combustion products could contain much (about 39%) soot and 61% gaseous species, most of which are hydrogen (about 30%) and methane (about 22%). The maximal pressure ratios measured in [1] were considerably less (~ 1.6) than the thermodynamic pressure ratio (6.21), which was the indication of incomplete oxidation of the test mixture. Among possible reasons of incomplete oxidation could be imperfect mixing of *n*-butane with oxygen and flame quenching caused by radical recombination on suspended and deposited soot particles, buoyancy effects, and heat loss. The effects produced by these imperfections are discussed below.

Table 1: Thermodynamic temperature, pressure, density, molecular mass, and species mole fractions at constant-pressure combustion (HP-problem) of the test mixture at p_0 = 4.1 bar and $T_0 = 500$ K

T, K	p, bar	r, kg/m^3	m, kg/kmol	Gaseous species					Soot
				H_2	CH_4	H_2O	CO	CO_2	
911.63	4.1	0.9508	10.361	32.16	19.43	6.12	1.42	0.58	40.28

Table 2: Thermodynamic temperature, pressure, density, molecular mass, and species mole fractions at constant-volume combustion (UV-problem) of the test mixture at p_0 = 4.1 bar and $T_0 = 500$ K

T, K	p, bar	r, kg/m^3	m, kg/kmol	Gaseous species					Soot
				H_2	CH_4	H_2O	CO	CO_2	
1049.42	25.47	5.2341	10.792	30.11	22.31	5.61	2.40	0.53	39.03

2. Mixture preparation

To understand the mixing dynamics of oxygen and *n*-butane in the 20-liter explosion vessel, 2D RANS-based simulations were performed using AVL SWIFT code [5]. In the calculations, the flow dynamics in the oxygen canister, in the manifold connecting the canister and the vessel, and in the vessel itself were simulated. After valve closing, only the dynamics of the flow in the vessel and in the manifold section downstream from the valve was considered with due regard for the gravity force effects. The geometrical dimensions of the 20-liter vessel, 0.6-liter oxygen canister and connecting manifolds were taken close to the design drawings. Contrary to similar CFD simulations of [3] without massive ignition electrodes, the ignition electrodes were added to the computational model reported herein. Three massive ignition electrodes, protruding from the upper flange of the vessel to the vessel center, were modeled by a hollow cylinder and an embodied coaxial cylindrical rod. All rigid walls of the computational volume were kept at constant temperature of 500 K, like in experiments [1]. The initial temperatures of oxygen and *n*-butane were also taken equal to 500 K to fit the experimental conditions of [1]. The turbulence model used in the simulations

was the standard $k-e$ model. The duration of oxygen injection was varied from 10 to 12 ms depending on the required experimental value of the final pressure of the mixture in the 20-liter vessel.

It was shown in [3] that oxygen injection in experiments [1] could lead to a considerable mixture stratification in terms of velocity, temperature and composition. The starting shock wave caused by a high initial pressure ratio (21 bar / 0.4 bar = 52.5) between the canister and the vessel was shown to be rather strong and resulted in high local flow velocities, exceeding 700 m/s in the jet core and attaining 400 m/s in the near-wall regions of the vessel.

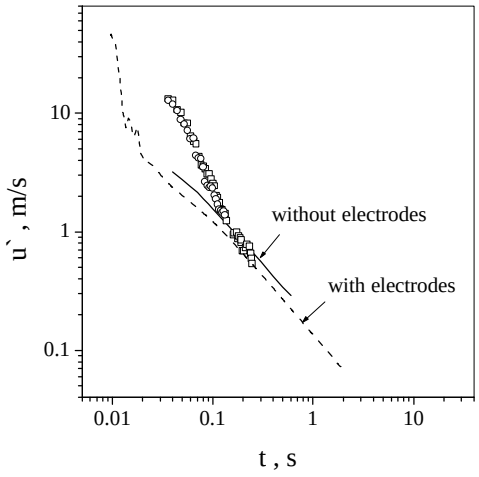

Figure 1: Comparison of predicted and measured [1] root-mean-squared velocity fluctuations *u*' in the vessel center. Initial oxygen pressure is 21 bar. Initial *n*-butane pressure is 0.4 bar. Injection duration is 0.0117 s. The solid line corresponds to calculations [3]. The dashed curve corresponds to present calculations

Figure 1 compares the predicted turbulent velocity in the vessel center with the root-mean-squared values of two pulsating velocity components measured in [1] using Laser Doppler Anemometry and with the computational results of [3]. It is seen that at $t > 0.1$ s, the predicted and measured results correlate reasonably well with each other, and the turbulence in [1] was isotropic at least at $t > 0.04$ s. At the initial injection stage, a large discrepancy between the predicted and measured data is observed, which could be explained by the failure of the standard $k-e$ model to simulate turbulence decay in the high-speed compressible flow.

Solid curves in Fig. 2 show the predicted time histories of oxygen mass fraction (Fig. 2*a*) and temperature (Fig. 2*b*) in the vessel center (ignition site) up to $t = 100$ s. For the sake of comparison, the time histories of mean oxygen mass fraction and mean temperature in the vessel are shown by the dashed curves in the same figures. In the computational runs relevant to Fig. 2, the oxygen injection period terminated at about $t = 0.01$ s. During injection, the oxygen mass fraction and temperature at the ignition site attained the values of 0.87 and 410 K, respectively. However, shortly after injection termination, the oxygen mass fraction and temperature attained the values of 0.117 and 500 K close to the corresponding mean values. Nevertheless, starting from $t = 3$–4 s, one can observe the deflection of the local oxygen mass fraction from the mean value in Fig. 2*a* (shown by arrow). The growth of the oxygen mass fraction in the vessel center continued till $t = 5$ s, when it attained a value of 0.14, and then turned to decrease gradually to the mean value of 0.117 at about $t = 100$ s.

The present results appeared to be somewhat different from the computational results of [3] without electrodes. Figure 3 compares the present results with the calculations of [3] in terms of the predicted oxygen mass fraction and temperature in the vessel center. Clearly, the values of oxygen mass fraction and temperature at the ignition site during oxygen injection differ considerably. However, after injection termination, the effect of electrodes is not much pronounced.

The reason for the elevated values of the oxygen mass fraction in the vessel center at $3 < t < 100$ s is evident from Fig. 4 showing the calculated distributions of the oxygen mass fraction (left hemisphere) and temperature (right hemisphere) at time (*a*) 3 s; (*b*) 10; (*c*) 20;

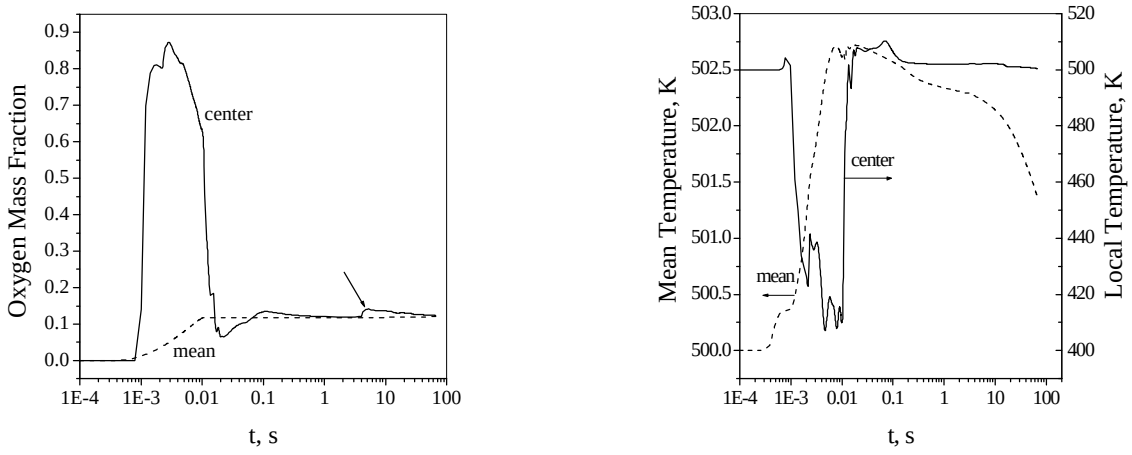

(*a*) (*b*)

Figure 2: Calculated time histories of (*a*) oxygen mass fraction and (*b*) temperature in the 20-liter vessel. Solid curves correspond to local instantaneous values at the ignition site (vessel center). Dashed curves correspond to mean values. Initial oxygen pressure in the canister is 29.67 bar. Initial *n*-butane pressure in the vessel is 3.2 bar. Injection duration is 0.01 s

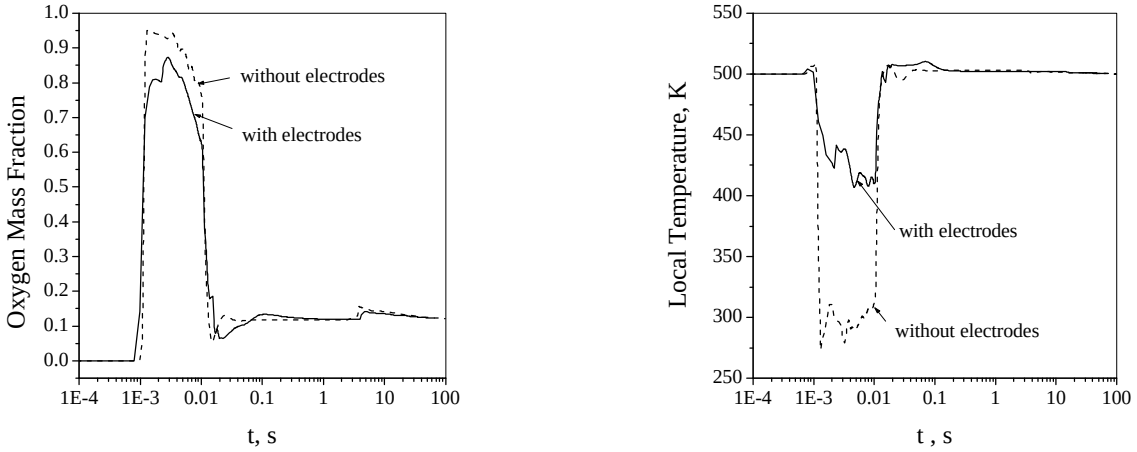

(*a*) (*b*)

Figure 3: Calculated time histories of oxygen mass fraction (*a*) and temperature (*b*) in the center of the 20-liter vessel. Solid curves correspond to the present calculations with taking the effect of ignition electrodes into account. Dashed curves correspond to calculations of [3] without electrodes. Initial oxygen pressure in the canister was 29.67 bar. Initial *n*-butane pressure in the vessel was 3.2 bar. Injection duration was 0.01 s

and (*d*) 100 s after oxygen injection termination. It is seen that at t = 3 s the mixing in the bulk of the vessel had been already completed. However, at this time there was still a portion of oxygen stagnated in the manifold at the instant of valve closing. This residual oxygen spread slowly along the injection axis. At time of about 3 s, the mass fraction of oxygen started to increase in the vessel center due to arrival of the residual oxygen from the manifold. Moreover, contrary to the calculations of [3] without electrodes, the present calculations indicated that some injected oxygen was accumulated in the space between the electrodes. It is seen from Fig. 4, that even at t = 100 s, the oxygen mass fraction in the space between the

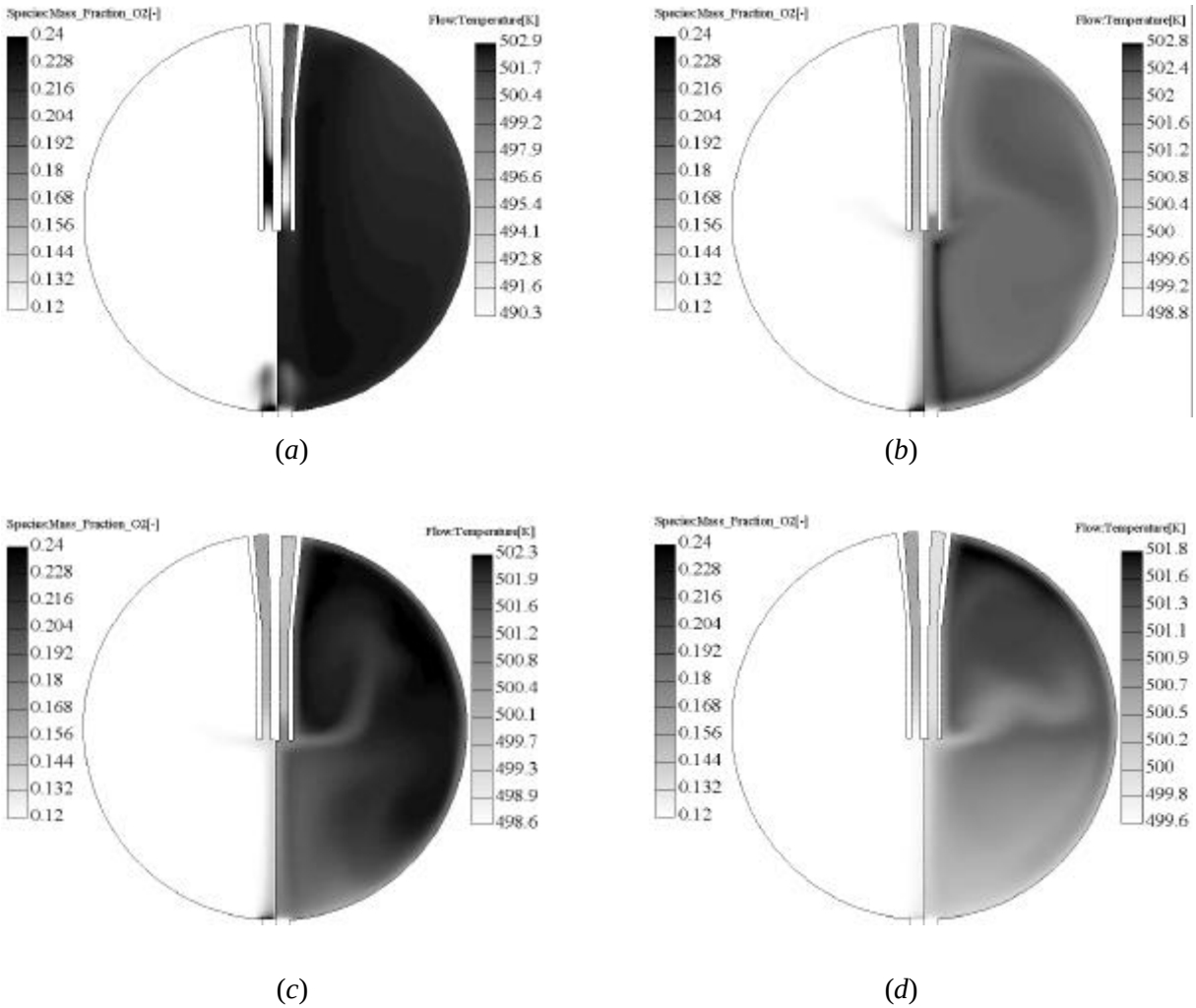

Figure 4: Calculated isolines of oxygen mass fraction (left hemisphere) and temperature (right hemisphere) at time (*a*) 3 s; (*b*) 10; (*c*) 20; and (*d*) 100 s after oxygen injection termination. Initial oxygen pressure was 29.67 bar. Initial *n*-butane pressure was 3.2 bar. Injection duration was 0.01 s

electrodes was considerably higher than the mean value. Of course, the coaxial electrodes in the present calculations served as a rough approximation of the complex 3D configuration of the realistic electrodes in the 20-liter vessel. However the additional calculations made with ring-shaped electrodes allowing oxygen to escape through the gaps have also demonstrated the effect of oxygen accumulation in the space between the electrodes, presumably due to effective stagnation of the oxygen jet in this blocked flow region. These findings are very important for understanding the results of experiments [1] with forced ignition of excessively fuel rich *n*-butane–oxygen mixture.

Thus, the CFD simulation of the mixing process in the 20-liter vessel provided a possible explanation for the local maximum of explosion pressure at about $t = 40$ s. This could be a result of ignition of a less fuel-rich (and therefore more reactive) *n*-butane–oxygen mixture than the test mixture with $\Phi = 23$.

4. Laminar flame propagation in test mixture

To estimate the reactivity of the test mixture in terms of the laminar burning velocity and the self-ignition delay, a detailed reaction mechanism of *n*-butane oxidation developed and

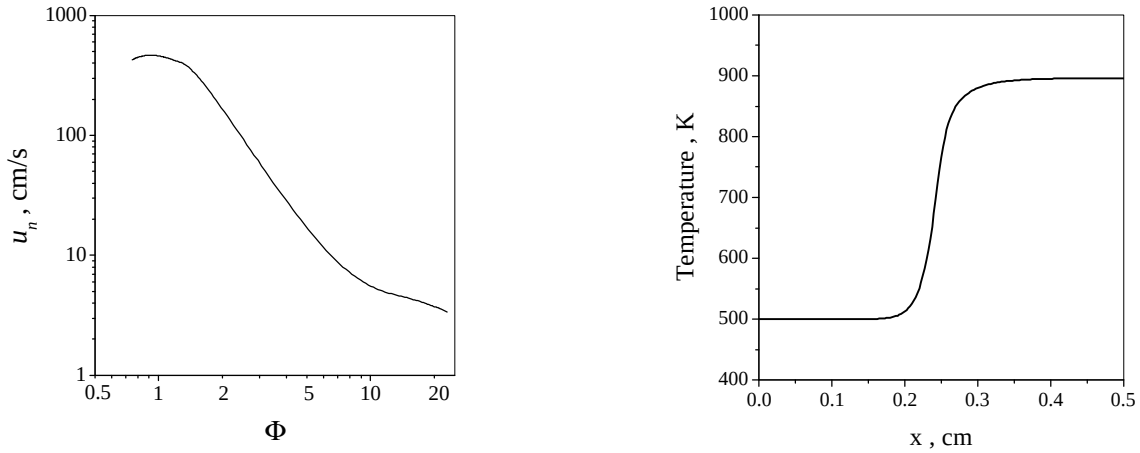

(*a*) (*b*)

Figure 5: (*a*) Predicted laminar burning velocities of *n*-C_4H_{10}–O_2 mixtures as a function of equivalence ratio Φ at T_0 = 500 K and p_0 = 4.1 bar; (*b*) Calculated temperature profile in the *n*-C_4H_{10}–O_2 laminar flame at Φ = 23 at T_0 = 500 K and p_0 = 4.1 bar

validated recently by the authors [6] was used. The mechanism contained 288 reversible elementary reactions and 54 species and was capable of simulating reasonably well both low- and high-temperature self-ignition of *n*-butane. At low temperatures and high pressures, this mechanism provided the parametric domain with the negative temperature coefficient of the reaction rate correlating well with experimental data [7]. It is worth mentioning however that this mechanism did not include reactions responsible for soot formation.

Figure 5*a* shows the predicted laminar burning velocity in the *n*-butane–oxygen mixture as a function of the equivalence ratio Φ under initial pressure and temperature conditions relevant to the experiments of [1]. The laminar burning velocity was calculated using the laminar flame code [8] assuming adiabatic walls and neglecting radiation heat loss. It is seen from Fig. 5*a* that the test mixture with Φ = 23 exhibited a laminar burning velocity u_n of 3.4 cm/s at T_0 = 500 K and p_0 = 4.1 bar, which was by two orders of magnitude less than the value of u_n for the stoichiometric *n*-butane–oxygen mixture at similar initial conditions (458 cm/s).

Figure 5*b* shows the calculated temperature profile in the laminar flame at Φ = 23. The temperature in the flame increased from $T_0 = 500$ K to about 896 K. The predicted flame temperature was somewhat less than the thermodynamic value of 911 K (see Table 1). The arising discrepancy was evidently caused by the lack of thermodynamic equilibrium at short distances behind the flame front shown in Fig. 5*b*.

The results of calculations presented in this section indicate that the test mixture in experiments [1] was flammable indeed.

5. Self-ignition of test mixture

As follows from Tables 1 and 2 oxidation and combustion of the test mixture should be accompanied by considerable soot formation. Under extremely fuel-rich experimental conditions [1], the contribution of chain termination reactions at soot particles deposited on the vessel walls and suspended in the mixture could be significant. In experiments [1], the existence of soot deposits on the vessel walls could be caused by incomplete air-blast removal of particles formed in previous tests. As for the origin of suspended soot particles in the vessel

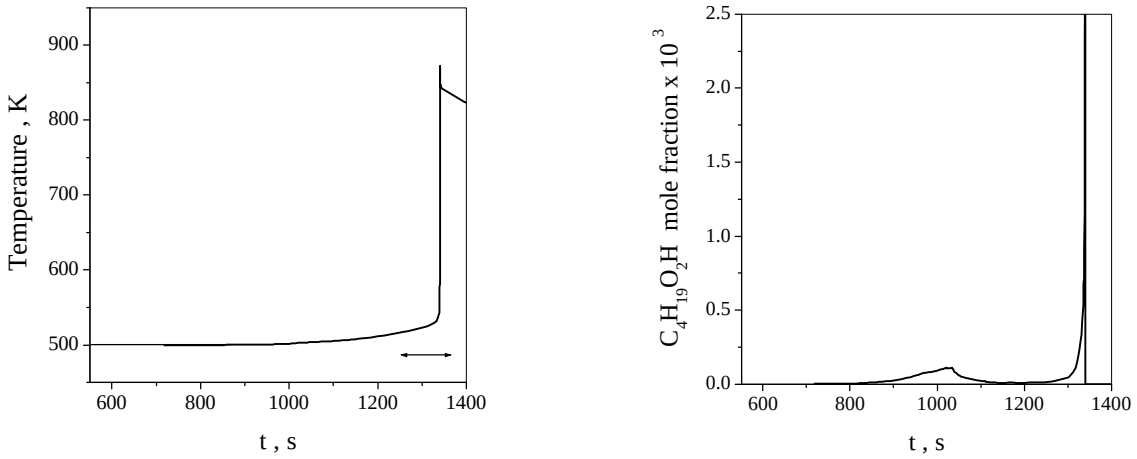

(*a*) (*b*)

Figure 6: (*a*) Predicted temperature history in the 78%C_4H_{10} +22%O_2 test mixture in the course of self-ignition at T_0 = 500 K and p_0 = 4.1 bar (arrow shows the experimental self-ignition delay); (*b*) Predicted time history of butyl hydroperoxide mole fraction in the test mixture

volume, they could be blown in the volume from the vessel walls by a strong starting shock wave (see Section 2), or could form in the mixture during the induction period according to a low-temperature mechanism of soot formation [9].

To model test mixture self-ignition at the conditions relevant to the experiments [1], the detailed reaction mechanism of *n*-butane oxidation [6] was used. Due to the lack of reliable information on kinetics of low-temperature heterogeneous reactions on the surface of soot particles, it was assumed that the most important chain termination reactions were represented by two overall, quasi-volumetric, monomolecular reactions [10]:

$$C_4H_9O_2H \rightarrow C_4H_{10} + O_2 \quad (1)$$

$$H_2O_2 \rightarrow H_2O + 0.5O_2 \quad (2)$$

The effective activation energies E_1 and E_2 of reactions (1) and (2) were taken zero, while the corresponding preexponential factors were taken equal to $k_1 = k_2 = k = 80$ s^{-1}. Figure 6*a* shows the results of calculations for the test mixture. The heat transfer coefficient in the calculations was taken equal to 0.615 W/m^{2}K. The arrow shows the experimentally measured self-ignition delays in [1].

It is seen from Fig. 6*a* that the predicted and measured ignition delays correlate well with each other. Note that the assumed value of $k \approx 80$ s^{-1} seemed quite reasonable for the problem under study. Note also that the increase of the heat transfer coefficient by the order of magnitude did not exert a significant effect on the computational results.

The calculations revealed the existence of a cool-flame stage during test mixture oxidation. The temperature curve in Fig. 6*a* exhibits a staged behavior with the first stage attributed to cool flame and the second to hot explosion. Figure 6*b* shows the corresponding time histories of butyl hydroperoxide mole fraction in the test mixture, which exhibits two stages of peroxide accumulation and decomposition at 800–1100 s and at 1200–1340 s, corresponding to the cool flame and hot explosion stages.

It is worth noting that the origin of cool flame ($t \approx 1000$ s) coincided well with the second maximum of the explosion pressure in the experiments of [1]. At the cool-flame stage

of hydrocarbon oxidation, the mixture reactivity is known to increase considerably [11]. Therefore, the second maximum at the explosion pressure curve could be explained by faster flame propagation in the test mixture at its ignition during the cool-flame conversion.

6. Effect of buoyancy

Slow burning mixtures are known to exhibit a strong influence of buoyancy effects [11]. Figure 7 shows the results of CFD simulations of upward natural convection of the hot ignition kernel in the gravity field. In this example, the mixture was ignited 10 s after termination of oxygen injection. These calculations were aimed at estimating the characteristic times taken for the kernel to reach the upper wall of the vessel and to cool down to the wall temperature. Combustion reactions in these calculations were not activated for the sake of simplicity.

It follows from Fig. 7 that the entire process of flame kernel dissipation took 1–2 s. If one takes into account that in actual experiments [1] the flame kernel moved upward along the massive electrodes, no wonder that combustion in [1] was incomplete and the maximal explosion pressure did not exceed a value of about 1.6 instead of the thermodynamic value of 6.21. Nevertheless, the present CFD simulations indicated that the flame kernel moved

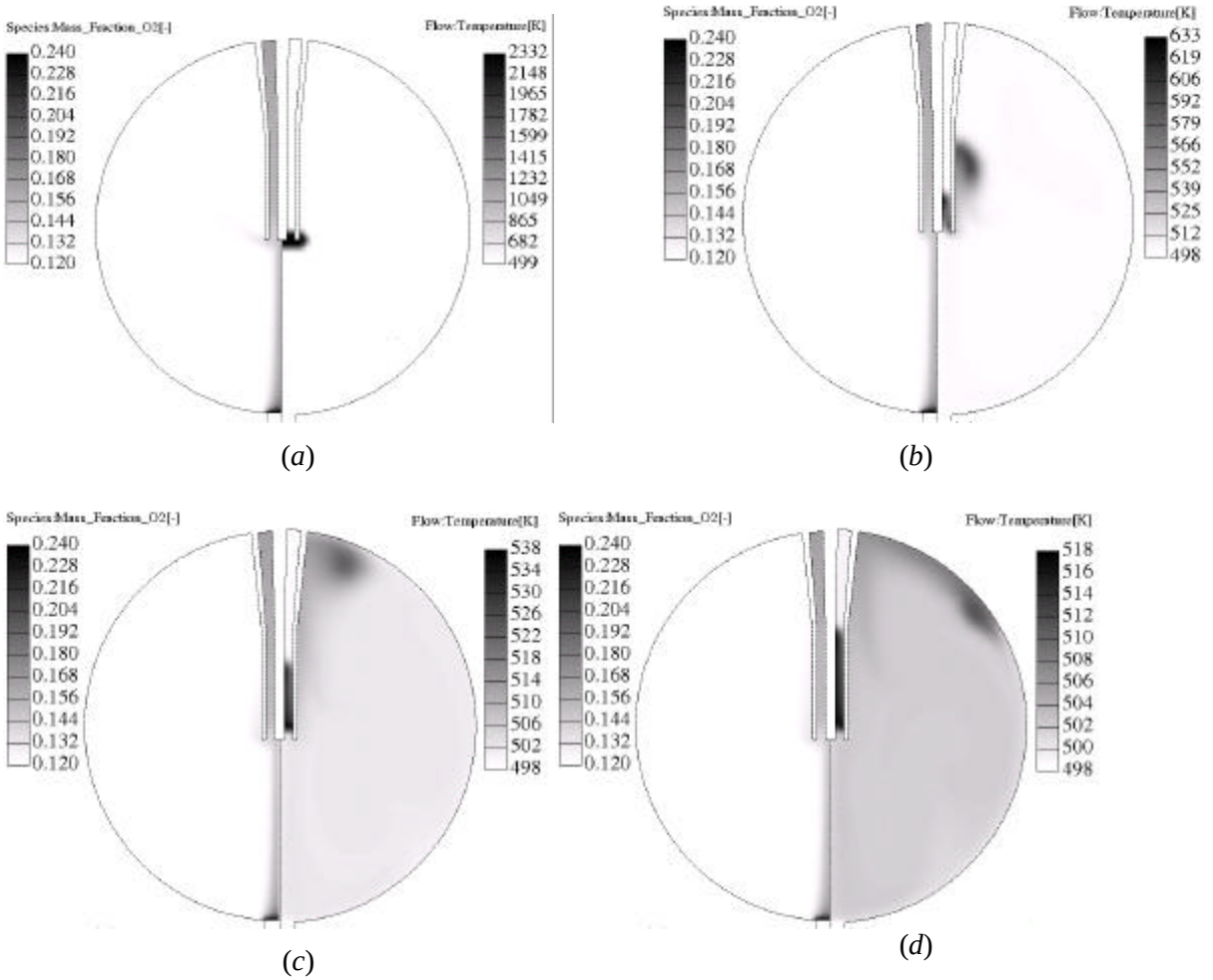

Figure 7: Calculated fields of oxygen mass fraction (left hemisphere) and temperature (right hemisphere) after ignition of test mixture in the vessel center 10 s after termination of oxygen injection: (*a*) ignition completion; (*b*) 0.3 s; (*c*) 1; and (*d*) 2 s after ignition. Initial oxygen pressure in the canister is 29.67 bar. Initial *n*-butane pressure in the vessel is 3.2 bar. Injection duration is 0.01 s. The interval between the isolines is uniform

upwards in the region with the elevated local oxygen concentration as compared to its mean value in the vessel.

7. Discussion and Conclusions

Experimental studies [1] of constant-volume combustion of the extremely fuel-rich 78% C_4H_{10} + 22% O_2 mixture (an equivalence ratio of 23) in the standard 20-liter vessel at elevated initial temperature (500 K) and pressure (4.1 bar) resulted in some unexpected phenomena, which needed explanation. Contrary to a standard testing procedure, a fuel–oxygen mixture in [1] was prepared by fast injection of oxygen from the pressurized canister to the explosion vessel filled with fuel. The mixture was ignited in the vessel center after different delay times (from several seconds to 1400 s) after completion of oxygen injection. It was found in [1] that the forced IDT affected considerably the explosion pressure and the maximum rate of pressure rise. The explosion pressure ratio was shown to increase with increasing the IDT to a maximum at an IDT of 40 s. After the maximum, the explosion pressure ratio dropped with increasing the IDT, reached a minimum at an IDT of 360 s and rose again to a second maximum at an IDT of 1020 s. Starting from about 1220 s, the test mixture self-ignited.

Based on the CFD simulations of the mixing process and natural convection of the ignition kernel, as well as on the analysis of the detailed reaction mechanism of *n*-butane oxidation, laminar flame propagation, and self-ignition, possible explanations for the phenomena observed in [1] can be suggested.

The test mixture was found to be flammable. At the initial conditions of [1], the mixture exhibited the laminar burning velocity of about 3.4 cm/s and the thermodynamic temperature of combustion products of 911.63 K. Self-ignition of the test mixture exhibited a two-stage behavior with a cool flame and hot explosion arising at about 1000 and 1300 s, respectively, after oxygen injection termination. Since the burning velocity of the test mixture was very low, its combustion in the vessel after forced ignition was highly affected by buoyancy. According to the estimations, the buoyant flame kernel could dissipate completely during 1–2 s after ignition due to the contact with massive electrodes and the upper wall of the vessel. As a result, combustion of the test mixture in [1] was always incomplete: a maximal explosion pressure ratio was only ~1.6 instead of the thermodynamic value of 6.21. Thus, the behavior of the explosion pressure ratio in the experiments [1] could be explained primarily by the variation of the laminar burning velocity in the test mixture with increasing the IDT. Keeping in mind the buoyant flame quenching in 1–2 s after ignition, one could expect that a higher explosion pressure ratio be attained at a higher burning velocity.

The mixture preparation procedure used in [1] implied a possibility of obtaining excessive (as compared to the mean value) oxygen concentration at the ignition site and in the space between the electrodes at a time between 3 and 100 s after injection termination. A higher oxygen concentration in a fuel-rich mixture implied a higher burning velocity (see Fig. 5*a*). This could be a reason for the first maximum at the explosion pressure curve, obtained in [1] at an IDT of about 40 s. Further temporal relaxation of the oxygen mass fraction in the vessel center and in the space between the electrodes to the mean value resulted in decreasing the burning velocity and the maximal explosion pressure to the minimal value at an IDT of about 360–400 s.

The subsequent increase in the maximal explosion pressure with the IDT exceeding 360–400 s could be explained by the growing influence of preflame reactions leading to formation of various intermediate combustion products including alkyl peroxides. As mixture reactivity is known to increase due to these processes, the laminar burning velocity in the preconditioned test mixture should also increase. Thus, the second maximum of the explosion pressure arising in [1] at an IDT of 1000 s could be explained by faster flame propagation in

the test mixture at its forced ignition during the cool-flame conversion. Further decrease of the maximal explosion pressure at an IDT exceeding 1000 s could be explained by lower reactivity and exothermicity of the test mixture. As a matter of fact, cool-flame conversion results in releasing of up to 7%–10% of available chemical energy in the test mixture. Therefore both the combustion temperature and the laminar burning velocity of the mixture passed through cool-flame oxidation should decrease. Forced ignition of such a mixture then should result in a lower explosion pressure.

Self-ignition of the test mixture at time exceeding 1220 s could be expected to result in the third prominent maximum of the explosion pressure ratio, caused by volumetric hot explosion (see Fig. 6*a*). However the corresponding experimental data in [1] do not seem to have it. It could be expected that at t = 1220–1380 s hot explosion in experiments [1] occurred locally in exothermic centers and therefore the resultant explosion pressure was still lower than at forced ignition. This implication is substantiated by the highest maximum rates of pressure rise relevant to self-ignition detected in [1]. Nevertheless, to verify this implication, further experimental and computational studies are required.

In general, the results of the study clearly indicate that apparently inflammable mixtures can nevertheless become hazardous depending on the mixture preparation procedure and forced ignition timing.

Acknowledgements

The work was partly supported by the Russian–Dutch Research Cooperation project No. 046.016.012 and Russian Foundation for Basic Research projects 05-08-50115a and 05-08-33411a.

References

1. Pekalski, A. A., Terli, E., Zevenbergen, J. F., Lemkowitz, S. M., & Pasman, H. J. (2005) Combustion Institute Proceedings, 30. 1133–1139.
2. Smetanyuk, V. A., Skripnik, A. A., Frolov, S. M., & Pasman, H. J. (2005) In G. D. Roy, S. M. Frolov, & A. M. Starik (Eds.), *Nonequilibrium Processes. Vol. 1: Combustion and Detonation* (pp. 37–43). Moscow:Torus Press.
3. Frolov, S. M., Basevich, V. Ya., Smetanyuk, V. A., Belyaev, A. A., & Pasman, H. J. (2006) Oxidation and combustion of fuel-rich*n*-butane–oxygen mixture in a standard 20-liter explosion vessel. European Conference on Computational Fluid Dynamics, ECCOMAS CDF 2006, P. Wesseling, E. Oñate, J. Périaux (Eds), Delft, The Netherlands: TU Delft.
4. Victorov, S. B. (2002) Proc. 12th International Detonation Symposium.
5. SWIFT Manual 3.1, AVL AST, AVL List GmbH, Graz, Austria (2002).
6. Basevich, V. Ya., Belayev, A. A., & Frolov, S. M. (2006, accepted) *Rus. J. Chemical Physics*.
7. Minetti, R., & Sochet, R. (1994) *Combustion and Flame, 96*. 201.
8. Belyaev, A. A., & Posvianskii, V. S. (1985) In: *Algorithms and Codes*. Information Bulletin of USSR Foundation of Algorithms and Codes. No. 3. 35.
9. Bohm, H., Hesse, D., *et al.* (1988) Proc. 22nd Symposium (Intern.) on Combustion. 403.
10. Kondratiev, V. N., & Nikitin, E. E. (1974) *Kinetics and Mechanism of Gas-Phase Reactions*, Moscow: Nauka.
11. Sokolik, A. S. (1960) *Self-Ignition, Flame, and Detonation in Gases*, Moscow: USSR Acad. Sci. Publ.